PHYSICAL REVIEW A **80**, 062506 (2009)

Comparative studies of dipole polarizabilities in Sr$^+$, Ba$^+$, and Ra$^+$ and their applications to optical clocks

B. K. Sahoo,[1,*] R. G. E. Timmermans,[1] B. P. Das,[2] and D. Mukherjee[3]
[1]*KVI, University of Groningen, NL-9747 AA Groningen, The Netherlands*
[2]*Non-accelerator Particle Physics Group, Indian Institute of Astrophysics, Bangalore 560034, India*
[3]*Raman Center for Atomic, Molecular and Optical Sciences, IACS, Kolkata 70032, India*
(Received 2 November 2009; published 7 December 2009)

Static dipole polarizabilities are calculated in the ground and metastable states of Sr$^+$, Ba$^+$ and Ra$^+$ using the relativistic coupled-cluster method. Trends of the electron correlation effects are investigated in these atomic ions. We also estimate the Stark and black-body radiation shifts from these results for these systems for the transitions proposed for the optical frequency standards and compare them with available experimental data.

DOI: 10.1103/PhysRevA.80.062506 PACS number(s): 31.15.A−

I. INTRODUCTION

There have been a number of significant proposals for new optical clocks that are more accurate than the current standard; the Cs clock [1–3]. Singly charged ions are some of the prominent candidates in this category due to the remarkable advances in modern ion trapping and laser cooling techniques [1–4]. *S-D* transitions in Sr$^+$ [3,5], Yb$^+$ [6], Hg$^+$ [1,7], Ba$^+$ [8,9], and Ra$^+$ [10] can serve as clock transitions. It is necessary to estimate the shifts of the energy levels for these cases due to stray electromagnetic fields in order to determine the accuracies of these potential optical clocks. Knowledge of hyperfine structure constants, electric quadrupole moments, gyromagnetic constants, and polarizabilities are essential quantities that can be used to estimate various possible shifts [11]. In our previous studies, we have already calculated hyperfine structure constants and electric quadrupole moments for the above ions [12,13]. It is possible to find the gyromagnetic constants approximately using analytical approaches for different states [11]. There have been extensive studies of the hyperfine structure constants of the low-lying states in the above ions using the relativistic coupled-cluster (RCC) method [10,13–15]. A few calculations of polarizabilities in these ions using the sum-over-states approach have also been reported recently [10,16].

Both Ba$^+$ and Ra$^+$ have also been proposed as suitable candidates for atomic parity violation (APV) experiments [17,18]. Determination of polarizabilities depends on the electric dipole (E1) matrix elements and excitation energies. On the other hand, the determination of APV amplitudes also depends on E1 matrix elements and excitation energies. Therefore, studies of correlation effects in these properties involving quantities in these systems are also useful for the APV studies. In contrast to hyperfine structure constants where the explicit behavior of electron correlation has been studied elaborately, the same cannot be done for polarizabilities using the sum-over-states approach. Also, the sum-over-states approach considers only a limited number of states, mainly from the single excited states and misses out contributions from continuum, double excited states, normalization of the wave functions etc.

In this work, we have employed an *ab initio* method in the RCC framework to calculate dipole polarizabilities of Sr$^+$, Ba$^+$, and Ra$^+$. The roles of different types of electron correlation effects in determining these quantities are studied and comparisons between these results are given explicitly. Contributions arising from different types of excited states and normalization of the wave functions through the RCC method have also been evaluated. Using these results, we then estimate the Stark and black-body radiation shifts in these systems which will be useful for the proposed optical clock experiments in the ions mentioned above.

II. THEORY

The polarizability of a given state $|J_nM_n\rangle$ can be expressed by

$$\alpha_0^i = 2\sum_{m\neq n} C_i(J_n)\frac{|\langle J_n||D||J_m\rangle|^2}{E_n - E_m}$$
$$= 2\sum_{m\neq n} C_i(J_n)(-1)^{J_n-J_m}\frac{\langle J_n||D||J_m\rangle\langle J_m||D||J_n\rangle}{E_n - E_m}, \quad (2.1)$$

where the subscript 0 represents for the static values and angular momentum coefficients $[C_i(J_n)]$ for the scalar (with superscript 1) and tensor (with superscript 2) dipole polarizabilities are given as

$$C_1(J_n) = -\frac{1}{3(2J_n+1)}, \quad (2.2)$$

and

$$C_2(J_n) = \left[\frac{10J_n(2J_n-1)}{3(J_n+1)(2J_n+1)(2J_n+3)}\right]^2 \times(-1)^{J_n-J_m}\begin{Bmatrix} J_n & 1 & J_m \\ 1 & J_n & 2 \end{Bmatrix}, \quad (2.3)$$

respectively. *Es* are the energies of the corresponding atomic states.

By defining a modified wave function due to the dipole operator, *D*, we can rewrite the above expression as

---

[*] b.k.sahoo@rug.nl

$$\alpha_0^i(J_n) = \langle J_n\|\tilde{D}_i\|J_n^{(1)}\rangle + \langle J_n^{(1)}\|\tilde{D}_i\|J_n\rangle, \tag{2.4}$$

where

$$|J_n^{(1)}\rangle = \sum_{m\neq n} |J_m\rangle \frac{\langle J_m\|D\|J_n\rangle}{E_n - E_m} \tag{2.5}$$

appears as a first-order correction to the $|J_n\rangle$ state due to the dipole operator D. In the above expression, we also define an effective dipole operator as

$$\tilde{D}_i = C_i(J_n)(-1)^{J_n-J_m}D, \tag{2.6}$$

whose matrix element between the original and perturbed wave functions will give the dipole polarizabilities. Here the intermediate states, $|J_m\rangle$, have parities opposite to that of $|J_n\rangle$ and they have to satisfy the usual triangular condition for the vector operator D.

To avoid the sum-over-states approach in the determination of the polarizabilities, we avoid the explicit form of $|J_n^{(1)}\rangle$ that is given by Eq. (2.5). Instead, we obtain $|J_n^{(1)}\rangle$ by solving the following equation:

$$(H - E_n)|J_n^{(1)}\rangle = -D|J_n\rangle, \tag{2.7}$$

that is similar to the first order perturbative equation. Here H is the atomic Hamiltonian which in the present work is considered in the Dirac-Coulomb approximation

$$H = \sum_i [c\alpha \cdot p_i + (\beta - 1)c^2 + V_{nuc}(r_i)] + \sum_{i>j}\frac{1}{r_{ij}}, \tag{2.8}$$

where c is the velocity of light, α and β are the Dirac matrices and $V_{nuc}(r)$ is the nuclear potential.

For an atomic system with zero nuclear spin, the Stark shift to the second order in the presence of an electric field (quadratic Stark shift) for $|J_n,M_n\rangle$ state is given by [19]

$$\Delta W_E(J_n,M_n;E) = -\frac{1}{2}\alpha_0^1(J_n)E^2 - \frac{1}{4}\alpha_0^2(J_n)\frac{[3M_n^2 - J_n(J_n+1)]}{J_n(2J_n-1)}(3E_z^2 - E^2), \tag{2.9}$$

where E and E_z are the magnitudes of the externally applied electric field in any arbitrary and z directions, respectively.

For atomic systems with nonzero nuclear spin (I), the expression for hyperfine states are given by [19]

$$\Delta W_E(F_n,M_{F_n};E) = -\frac{1}{2}\alpha_0^1(F_n)E^2 - \frac{1}{4}\alpha_0^2(F_n) \times \frac{[3M_{F_n}^2 - F_n(F_n+1)]}{F_n(2F_n-1)}(3E_z^2 - E^2), \tag{2.10}$$

where $F_n = I + J_n$ and M_{F_n} are the total spin due to nuclear spin I and atomic state spin J_n and its azimuthal component, respectively. Since it is easier for us to deal with J_n of the electronic states, therefore we express all the above quantities in terms of electronic coordinate. By using the following relations [11]:

$$\alpha_0^1(F_n) = \alpha_0^1(J_n) \tag{2.11}$$

and

$$\alpha_0^2(F_n) = (-1)^{I+J_n+F_n}\alpha_0^2(J_n)\left[\frac{F_n(2F_n-1)(2F_n+1)}{(2F_n+3)(F_n+1)}\right] \times \left[\frac{(2J_n+1)(J_n+1)(2J_n+3)}{J_n(2J_n-1)}\right] \times \begin{Bmatrix} F_n & I & J_n \\ J_n & F_n & 2 \end{Bmatrix}, \tag{2.12}$$

between the dipole polarizabilities of the electronic and hyperfine states, we obtain

$$\Delta W_E(F_n,M_{F_n};E) = -\frac{1}{2}\alpha_0^1(J_n)E^2 - \frac{1}{4}(-1)^{I+J_n+F_n}\alpha_0^2(J_n)\left[\frac{3M_{F_n}^2 - F_n(F_n+1)}{F_n(2F_n-1)}\right]\left[\frac{F_n(2F_n-1)(2F_n+1)(2J_n+1)(J_n+1)(2J_n+3)}{(2F_n+3)(F_n+1)J_n(2J_n-1)}\right] \times \begin{Bmatrix} F_n & I & J_n \\ J_n & F_n & 2 \end{Bmatrix}(3E_z^2 - E^2). \tag{2.13}$$

Again, the blackbody-radiation (BBR) shift of a given state $|J_n,M_n\rangle$ in the adiabatic expansion due to the applied isotropic electric field radiated at temperature T [in Kelvin (K)] can be assumed as [20]

$$\Delta_{BBR} = -\frac{1}{2}(831.9\ \text{V/m})^2\left(\frac{T(\text{K})}{300}\right)^4\alpha_0^1(J_n). \tag{2.14}$$

III. METHOD OF CALCULATIONS

The RCC method, which is equivalent to all order perturbation theory, has been recently used to obtain precise results and account for the correlation effects accurately in single valence systems [10,12–15]. In the RCC framework, the wave function of a single valence atom can be expressed as

$$|\Psi_n^{(0)}\rangle = e^T\{1+S_n\}|\Phi_n\rangle, \tag{3.1}$$

where $|\Phi_n\rangle$ is the reference state constructed from the Dirac-Fock (DF) wave function $|\Phi_0\rangle$ of the closed-shell configuration by appending the corresponding valence electron as $|\Phi_n\rangle = a_n^\dagger|\Phi_0\rangle$ with $a_n^\dagger$ representing addition of a valence electron n. Here T and S_n are the RCC excitation operators which excite electrons from $|\Phi_0\rangle$ and $|\Phi_n\rangle$, respectively. The amplitudes of these excitation operators are obtained by the following equations

$$\langle\Phi^L|\{\widehat{H_N e^T}\}|\Phi_0\rangle = 0, \tag{3.2}$$

$$\langle\Phi_n^L|\{\widehat{H_N e^T}\}S_n|\Phi_n\rangle = -\langle\Phi_n^L|\{\widehat{H_N e^T}\}|\Phi_n\rangle + \langle\Phi_n^L|S_n|\Phi_n\rangle\Delta E_n, \tag{3.3}$$

with the superscript $L(=1,2)$ representing the single and double excited states from the corresponding reference states and the wide-hat symbol over $H_N e^T$ represent the linked terms of normal order atomic Hamiltonian H_N and RCC operator T. For the single and double excitations approximation (CCSD method), the corresponding RCC operators are denoted by

$$T = T_1 + T_2 \tag{3.4}$$

and

$$S_n = S_{1n} + S_{2n} \tag{3.5}$$

for the closed-shell and single valence configurations, respectively. Again, ΔE_n in the above expressions is the corresponding valence electron affinity [negative of the ionization potential (IP)] energy which is evaluated by

$$\Delta E_n = \langle\Phi_n|\{\widehat{H_N e^T}\}\{1+S_n\}|\Phi_n\rangle. \tag{3.6}$$

In Eq. (3.2), we have considered only the single and double excitations, however we have incorporated contributions from important triple excitations [CCSD(T) method] perturbatively in Eq. (3.3) by defining

$$S_{3n}^{pert} = \widehat{H_N T_2} + \widehat{H_N S_{2n}}, \tag{3.7}$$

where the superscript *pert* denotes for the perturbation, and evaluating their contributions to ΔE_n from these operators by

$$\Delta E_n^{trip} = \widehat{T_2^\dagger S_{3n}^{pert}}. \tag{3.8}$$

After obtaining the amplitudes for T, the core excitation operator, we solve Eqs. (3.3) and (3.6) simultaneously to obtain the amplitudes for the S_n operators.

We extend the RCC ansatz for the perturbed atomic state in the presence of the electric dipole operator D by writing the total atomic wave function as

$$|\widetilde{\Psi}_n\rangle = e^{T+\Omega}\{1+S_n+\Lambda_n\}|\Phi_n\rangle, \tag{3.9}$$

where Ω and Λ_n are the first order corrections to the RCC operators T and S_n, respectively. Since Eq. (2.7) is first order in the operator D, the above expression will reduce to

$$|\widetilde{\Psi}_n\rangle = e^T\{1+S_n+\Omega(1+S_n)+\Lambda_n\}|\Phi_n\rangle. \tag{3.10}$$

Now, separating the above wave function as $|\Psi_n^{(0)}\rangle$ and $|\Psi_n^{(1)}\rangle$, we get

$$|\Psi_n^{(1)}\rangle = e^T\{\Omega(1+S_n)+\Lambda_n\}|\Phi_n\rangle. \tag{3.11}$$

Following Eq. (2.7), we solve again the amplitudes for the modified operators as

$$\langle\Phi^L|\{\widehat{H_N e^T \Omega}\}|\Phi_0\rangle = -\langle\Phi^L|\widehat{De^T}|\Phi_0\rangle, \tag{3.12}$$

$$\begin{aligned}\langle\Phi_n^L|\{\widehat{H_N e^T}\}\Lambda_n|\Phi_n\rangle = &-\langle\Phi_n^L|\{\widehat{H_N e^T}\Omega(1+S_n)+\widehat{De^T}(1+S_n)\}\\ &\times|\Phi_n\rangle + \langle\Phi_n^L|\Lambda_n|\Phi_n\rangle\Delta E_n,\end{aligned} \tag{3.13}$$

where $\widehat{De^T}$ represents the connecting terms between D and T operators. Again in our CCSD approximation, we have

$$\Omega = \Omega_1 + \Omega_2 \tag{3.14}$$

and

$$\Lambda_n = \Lambda_{1n} + \Lambda_{2n}. \tag{3.15}$$

Therefore, the RCC expression for the dipole polarizability is given by

$$\alpha_0^i = \frac{\langle\Psi_n^{(0)}|\widetilde{D}_i|\Psi_n^{(1)}\rangle + \langle\Psi_n^{(1)}|\widetilde{D}_i|\Psi_n^{(0)}\rangle}{\langle\Psi_n^{(0)}|\Psi_n^{(0)}\rangle} = \frac{\langle\Phi_n|\{1+S_n^\dagger\}\overline{\widetilde{D}}_i\{\Omega(1+S_n)+\Lambda_n\}|\Phi_n\rangle + \langle\Phi_n|\{\Lambda_n^\dagger + (1+S_n^\dagger)\Omega^\dagger\}\overline{\widetilde{D}}_i\{1+S_n\}|\Phi_n\rangle}{\langle\Phi_n|\{1+S_n^\dagger\}\bar{N}_0\{1+S_n\}|\Phi_n\rangle}, \tag{3.16}$$

where we define $\overline{\widetilde{D}_i} = (e^{T^\dagger}\widetilde{D}_i e^T)$ and $\bar{N}_0 = e^{T^\dagger}e^T$. The nontruncative series for $\widetilde{D}_i$ and $\bar{N}_0$ are expanded using the Wick's generalized theorem and truncated the series when the leading order nonaccounted terms are below fifth order of Coulomb interaction. These operators are then contracted with Ω to get fully contracted terms that give rise core electron contributions. The core-valence and valence correlation contributions are obtained from the open contraction between the operators with Ω and $\Omega\{1+S_n\}+\Lambda_n$ operators, respectively.

Corrections due to the normalization of the wave functions are accounted by evaluating

$$\text{Norm} = [\langle \Psi_n^{(0)} | \tilde{D}_i | \Psi_n^{(1)} \rangle + \langle \Psi_n^{(1)} | \tilde{D}_i | \Psi_n^{(0)} \rangle] \left\{ \frac{N_n}{1 + N_n} \right\}, \tag{3.17}$$

where $N_n = \langle \Phi_n | \{1 + S_n^{\dagger}\} \bar{N}_0 \{1 + S_n\} | \Phi_n \rangle$.

IV. RESULTS AND DISCUSSIONS

A. General discussions

The orbitals used in the present work are generated on a radial grid given by

$$r_i = r_0[e^{h(i-1)} - 1], \tag{4.1}$$

where i represents a grid point. The total number of grid points in our calculations is 750, the step size h is taken as 0.03 in the present case and r_0 is taken as 2×10^{-6} a.u. To construct the basis functions, we use Gaussian-type orbitals (GTOs) defined as

$$F^{GTO}(r_i) = r^{n_\kappa} e^{-\alpha_i r_i^2}. \tag{4.2}$$

Here n_κ is the radial quantum number of the orbitals and α_i is a parameter whose value is chosen to obtain orbitals with proper behavior inside and outside the nucleus of an atomic system. Further, the $\alpha_i s$ satisfy the even tempering condition

$$\alpha_i = \alpha_0 \beta^{i-1}. \tag{4.3}$$

We have chosen same $\alpha_0 = 0.005\,25$ and $\beta = 2.73$ values to construct the basis functions in Sr^+, Ba^+, and Ra^+, so that effects due to the different sizes of the systems can be compared. Finite size of the nucleus in these systems are accounted by assuming a two-parameter Fermi-nuclear-charge distribution for evaluating the electron density over nucleus as given by

$$\rho(r_i) = \frac{\rho_0}{1 + e^{(r_i - c)/a}}, \tag{4.4}$$

where c and a are the half-charge radius and skin thickness of the nucleus. These parameters are chosen as

$$a = 2.3/4(\ln 3) \tag{4.5}$$

and

$$c = \sqrt{\frac{5}{3} r_{rms}^2 - \frac{7}{3} a^2 \pi^2}, \tag{4.6}$$

where r_{rms} is the root mean square radius of the corresponding nuclei which is determined as discussed in [21].

In Table I, we present our DF and CCSD(T) results along with other available calculations and experimental results for the dipole polarizabilities of the ground and metastable states of Sr^+, Ba^+, and Ra^+. The differences between the DF and CCSD(T) results indicate the magnitudes of the electron correlation effects in the determination of the dipole polarizabilities in these systems using the CCSD(T) method. They are 45%, 48%, and 58% for the ground states of Sr^+, Ba^+, and Ra^+, respectively. They increase with the size of the system. However, the correlation effects in the $d_{3/2}$ metastable states are 137%, 85%, and 119% for the scalar polarizabilities and 159%, 83%, and 128% for the tensor polarizabilities in Sr^+, Ba^+, and Ra^+, respectively. This shows that the correlation effects reduce in these states from Sr^+ to Ba^+, but the presence of the core *f*-orbitals increases the correlation effects in Ra^+. The correlation effects in the $d_{5/2}$ metastable states are 117%, 73% and 75% for the scalar polarizabilities and 138%, 88%, and 87% for the tensor polarizabilities in Sr^+, Ba^+, and Ra^+, respectively. This implies that the correlations in the *d*-metastable states do not depend upon the size but the internal structure of the systems. Our previous studies on the hyperfine structure constants in these systems [10,13–15] had shown peculiar behavior of the core-polarization effects. These effects were comparatively smaller in the $d_{3/2}$ metastable states. In contrast, the correlation effects are larger in the $d_{3/2}$ metastable states compared to the $d_{5/2}$ metastable states and the ground states in the dipole polarizabilities calculations.

The upper limits to the error bars in these quantities were determined by taking the differences of the results obtained using CCSD(T) and CCSD methods and the inaccuracies due to the self-consistent results obtained at the DF levels by varying the number of GTOs considered in the calculations. These results are quoted inside the parentheses in Table I.

We explicitly present the diagrams in Fig. 1 corresponding to various RCC terms that are significant in determining the dipole polarizabilities. As seen from the figure, Fig. 1(a) which arises from the fully contracted terms of $\bar{\bar{\tilde{D}}}\Omega_1$ corresponds to the core-correlation contributions. Its lower-order terms correspond mainly to the diagrams coming from the random-phase approximation (RPA). There are also core-correlation contributions arising from $\bar{\bar{\tilde{D}}}\Omega_2$, but they are relatively small and are not shown in Fig. 1. The core-valence correlation contributions are determined by open diagrams from $\bar{\bar{\tilde{D}}}\Omega_1$ as shown in Fig. 1(b). The most important correlation contributions arise through the valence correlation effects and they are shown in Figs. 1(c) and 1(d). Important pair-correlation and core-polarization effects are accounted through $\bar{\bar{\tilde{D}}}\Lambda_{1n}$, however core-polarization effects arising from the perturbed doubly excited states are accounted through $\bar{\bar{\tilde{D}}}\Lambda_{2n}$. The DF contributions involving the core, core-valence and virtual orbitals are the lowest order diagrams to the fully contracted $\bar{\bar{\tilde{D}}}\Omega_1$, open $\bar{\bar{\tilde{D}}}\Omega_1$ and $\bar{\bar{\tilde{D}}}\Lambda_{1n}$ RCC terms, respectively. Based on the above mentioned correlation diagrams, we analyze their roles in different systems considered below.

B. Sr^+

There are no experimental results of the dipole polarizabilities available for the ground and metastable excited states in Sr^+. However, a number of calculations have been carried out using different methods and we have compared their results with the present work in Table I. Lim and Schwerdtfeger [22] have done comparative studies between the nonrelativistic and scalar relativistic Douglas-Kroll calculations using four different many-body methods. They

TABLE I. Comparison of dipole polarizabilities between different works in Sr^+, Ba^+ and Ra^+ (in atomic unit). Abbreviations: HF → Hartree-Fock, nonrel. → nonrelativistic, DK rel. → scalar relativistic Douglas-Kroll method, MBPT(2) → second order perturbation theory, sum-over → sum-over intermediate states.

	$ns_{1/2}$	$(n-1)d_{3/2}$		$(n-1)d_{5/2}$			
System	α_0^1	α_0^1	α_0^2	α_0^1	α_0^2	Methods	References
$Sr^+(n=5)$							
	127.62	145.86	−91.81	136.84	−116.02	DF	This work
	88.29(1.0)	61.43(52)	−35.42(25)	62.87(75)	−48.83(30)	CCSD(T)	This work
	132.15					HF	[22]
	86.21					nonrel. MBPT(2)	[22]
	101.58					nonrel. CCSD	[22]
	97.91					nonrel. CCSD(T)	[22]
	121.33					DK DF	[22]
	79.89					DK rel. MBPT(2)	[22]
	94.31					DK rel. CCSD	[22]
	91.10					DK rel. CCSD(T)	[22]
	91.3(9)			62.0(5)	−47.7(3)	LCCSD(T) + sum-over	[16]
	89.88			61.77		Nonrel. + sum-over	[23]
	93.3			57.0		Nonrel. + sum-over	[24]
	84.6(3.6)			48(12)		Nonrel. + sum-over	[5]
	91.47					Nonrel. + sum-over	[25]
	86(11)					Experiment + nonrel.	[26]
$Ba^+(n=6)$							
	184.49	90.07	−45.07	87.66	−58.02	DF	This work
	124.26(1.0)	48.81(46)	−24.62(28)	50.67(58)	−30.85(31)	CCSD(T)	This work
	213.47					HF	[22]
	110.60					nonrel. MBPT(2)	[22]
	148.24					nonrel. CCSD	[22]
	146.88					nonrel. CCSD(T)	[22]
	177.64					DK DF	[22]
	94.64					DK rel. MBPT(2)	[22]
	129.92					DK rel. CCSD	[22]
	123.07					DK rel. CCSD(T)	[22]
	124.15					LCCSD(T) + sum-over	[29]
	124.7					Nonrel. + sum-over	[25]
	126.2					Nonrel. + sum-over	[30]
	123.88(5)					Experiment	[27]
	125.5(10)					Experiment	[28]
$Ra^+(n=7)$							
	164.66	183.07	−114.70	143.77	−98.64	DF	This work
	104.54(1.5)	83.71(77)	−50.23(43)	82.38(70)	−52.60(45)	CCSD(T)	This work
	257.00					HF	[22]
	123.23					non-rel. MBPT(2)	[22]
	186.23					nonrel. CCSD	[22]
	172.00					nonrel. CCSD(T)	[22]
	145.47					DK DF	[22]
	79.80					DK rel. MBPT(2)	[22]
	110.48					DK rel. CCSD	[22]

TABLE I. (*Continued.*)

	$ns_{1/2}$	$(n-1)d_{3/2}$		$(n-1)d_{5/2}$			
System	α_0^1	α_0^1	α_0^2	α_0^1	α_0^2	Methods	References
	105.37					DK rel. CCSD(T)	[22]
	106.12	95.54	−55.06	91.85	−58.33	CCSD(T)+sum-over	[10]
	106.5					LCCSD(T)+sum-over	[32]
	106.22					LCCSD(T)+sum-over	[33]

demonstrate the importance of the relativistic methods to calculate dipole polarizabilities. Jiang *et al.* [16] have used E1 matrix elements obtained using the linearized RCC method with the singles, doubles, and partial triple excitations [LCCSD(T)] to evaluate the valence correlation contributions for a few intermediate states. The core correlations are accounted through the RPA method and contributions from higher states were estimated using the DF method. Mitroy *et al.* [23] have used a nonrelativistic method using the sum-over-states approach to determine polarizabilities of the ground and 4*d* states. As seen in Table I, the dipole polarizabilities of the $4d_{3/2}$ and $4d_{5/2}$ states are not the same and they cannot be evaluated separately using a nonrelativistic method. However, our ground state polarizability for Sr$^+$ agrees with their result. Similar approaches were also employed by Barklem and OMara [24]. Patil and Tang [25] have employed a summation and integration approach to determine the ground-state polarizability. Recently, Nunkaew *et al.* [26] have estimated E1 matrix elements using the nonrelativistic theory and microwave resonance measurements in Sr and have extracted dipole polarizability of the ground state of Sr$^+$.

In Table II, we present the individual contributions from RCC terms to the dipole polarizability calculations in Sr$^+$. Our core-correlation contributions are 4.98 and −0.27 a.u. for the scalar and tensor dipole polarizabilities, respectively. Clearly, the CCSD(T) result for the scalar dipole polarizability is smaller than the previously estimated values. On the other hand, the core correlation to the tensor polarizability vanishes in the nonrelativistic theory, but it is finite in our approach, although small in magnitude. Jiang *et al.* [16] have neglected this contribution in their calculations. We have also given DF results from the core ($\tilde{D}_c$) and virtual ($\tilde{D}_v$) orbitals separately in the same table. Our DF result and that reported by Lim and Schwerdtfeger [22] differ. Comparing our DF results given in Tables I and II, it seems that Lim and Schwerdtfeger have not included core-correlation contributions at the DF level. Again, the lowest order contributions to $\tilde{D}_c$ and $\tilde{D}_v\Lambda_{1n}$ terms correspond to $\tilde{D}_c$ and $\tilde{D}_v$, respectively. The differences between the lowest order and all order results seem to be significant in this system. The largest contribution to the final results comes from $\tilde{D}_v\Lambda_{1n}$ as it contains DF result due to virtual orbitals in it. Contributions from $\tilde{D}_v\Lambda_{2n}$ correspond to doubly excited perturbed states and they are also large in both the ground and metastable states. Therefore, the exclusion of these contributions in the sum-over-state approach may not be appropriate. Again, normalization corrections (Norm) are also non-negligible.

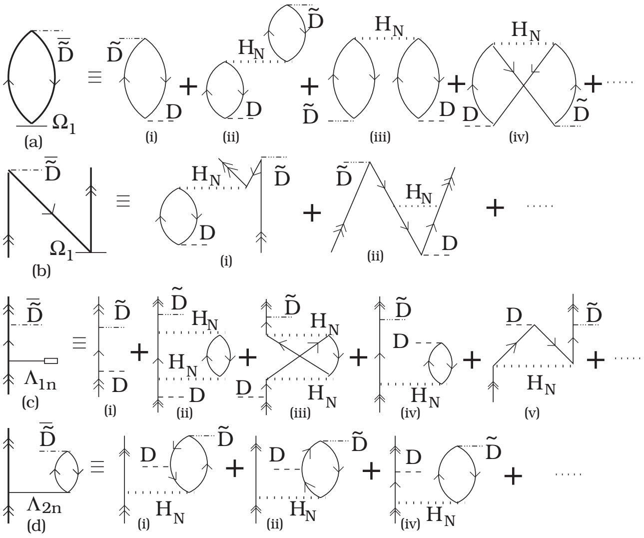

FIG. 1. Breakdown of RCC terms into lower-order perturbative diagrams. Lines with singles going up and down represent virtual and occupied orbitals, respectively. Lines with the double arrows represent valence orbital. Broken lines, dotted lines, and broken lines with dots are the bare dipole, two-body part of the Hamiltonian and effective one-body dipole operators, respectively.

C. Ba$^+$

Two experimental results with small uncertainties [27,28] are available for the ground state dipole polarizability in Ba$^+$. There have also been studies of this quantity by Lim and Schwerdtfeger [22]. Iskrenova-Tchoukova and Safronova [29] have employed E1 matrix elements from the LCCSD(T) method in the sum-over-states approach using a few states for the valence correlation effects and estimating the core-correlation and core-valence correlation contributions from lower-order perturbation theory to determine this quantity. Other available calculations [25,30] are based on nonrelativistic methods. Again, there are no other results available for the metastable *d* states in Ba$^+$ to compare with our results. However, we have also carried-out a sum-over-states calculation using the E1 matrix elements from the CCSD(T) method [31] that agrees with our *ab initio* results.

We present contributions from individual RCC terms to the dipole polarizabilities calculations on Ba$^+$ in Table III. The trends of these correlation effects seem to be the same as in Sr$^+$. However, the core-correlation effects in this system seem to be almost twice than in the case of Sr$^+$. The core-

TABLE II. Contributions from the DF and various CCSD(T) terms to the dipole polarizability calculations in Sr$^+$. The subscripts c, n, and v of the RCC terms correspond to the core, valence, and virtual correlation contributions. $\tilde{D}_c$ and $\tilde{D}_n$ give the DF results from the core and valence orbitals.

	$5s\ ^2S_{1/2}$	$4d\ ^2D_{3/2}$		$4d\ ^2D_{5/2}$	
Terms	α_0^1	α_0^1	α_0^2	α_0^1	α_0^2
$\tilde{D}_c$	6.15	6.15	−0.25	6.15	−0.25
$\underline{\tilde{D}_n}$	121.47	139.71	−91.56	130.69	−115.78
$\underline{\tilde{D}_c}$	4.98	4.98	−0.27	4.98	−0.27
$\underline{\tilde{D}_v}\Omega+cc$	0.10	0.20	−0.35	0.41	−0.41
$\underline{\tilde{D}_v}\Lambda_{1n}+cc$	93.78	67.05	−38.70	68.14	−56.54
$\tilde{D}_v\underline{\Lambda_{2n}}+cc$	−2.87	−2.54	−0.86	−2.43	1.72
$S_{1v}\underline{\tilde{D}_v}\Lambda_{1n}+cc$	−3.74	−6.06	3.47	−6.10	5.05
$S_{2v}\underline{\tilde{D}_v}\Lambda_{1n}+cc$	−3.03	−1.47	0.77	−1.39	0.96
$S_{1v}\underline{\tilde{D}_v}\Lambda_{2n}+cc$	−0.04	0.06	0.03	0.05	−0.03
$S_{2v}\tilde{D}_v\Lambda_{2n}+cc$	0.13	−0.05	0.03	−0.06	0.03
Others	0.13	0.22	−0.14	0.24	−0.15
Norm	−1.15	−0.96	0.60	−0.97	0.81

valence correlations coming through the open $\overline{\tilde{D}_v}\Omega$ diagrams are also larger than Sr$^+$. Contributions from the doubly excited perturbed states and corrections due to the normalization of the wave functions also seem to be significant.

D. Ra$^+$

There are also no experimental results available for the dipole polarizabilities in Ra$^+$. In the same work as mentioned above, Lim and Schwerdtfeger [22] have also calculated this quantity in the ground state of Ra$^+$ using various many-body methods. Safronova *et al.* [32,33] have also evaluated this result using the sum-over-states approach. Their valence correlation effects are evaluated using E1 matrix elements for a few important states from the LCCSD(T) method and core-correlation and core-valence correlations are evaluated using lower-order many-body methods. In our earlier work [10],

TABLE III. Contributions from the DF and various CCSD(T) terms to the dipole polarizability calculations in Ba$^+$. The subscripts c, n, and v of the RCC terms correspond to the core, valence, and virtual correlation contributions. $\tilde{D}_c$ and $\tilde{D}_n$ give the DF results from the core and valence orbitals.

	$6s\ ^2S_{1/2}$	$5d\ ^2D_{3/2}$		$5d\ ^2D_{5/2}$	
Terms	α_0^1	α_0^1	α_0^2	α_0^1	α_0^2
$\tilde{D}_c$	11.73	11.73	−0.46	11.73	−0.46
$\underline{\tilde{D}_n}$	172.76	78.33	−44.61	75.93	−57.56
$\underline{\tilde{D}_c}$	9.35	9.35	−0.56	9.35	−0.56
$\underline{\tilde{D}_v}\Omega+cc$	0.23	0.33	−0.64	0.82	−0.82
$\underline{\tilde{D}_v}\Lambda_{1n}+cc$	133.01	49.20	−25.61	50.17	−36.23
$\tilde{D}_v\underline{\Lambda_{2n}}+cc$	−4.93	−3.23	−1.36	−3.05	2.19
$S_{1v}\underline{\tilde{D}_v}\Lambda_{1n}+cc$	−6.58	−4.45	2.39	−4.42	3.37
$S_{2v}\underline{\tilde{D}_v}\Lambda_{1n}+cc$	−5.18	−1.98	0.84	−1.83	0.89
$S_{1v}\underline{\tilde{D}_v}\Lambda_{2n}+cc$	−0.06	0.05	0.03	0.03	−0.01
$S_{2v}\tilde{D}_v\Lambda_{2n}+cc$	0.27	−0.10	0.05	−0.09	0.06
Others	0.21	0.45	−0.25	0.49	−0.33
Norm	−2.06	−0.81	0.49	−0.80	0.59

TABLE IV. Contributions from the DF and various CCSD(T) terms to the dipole polarizability calculations in Ra$^+$. The subscripts c, n, and v of the RCC terms correspond to the core, valence and virtual correlation contributions. $\tilde{D}_c$ and $\tilde{D}_n$ give the DF results from the core and valence orbitals.

	$7s\ ^2S_{1/2}$	$6d\ ^2D_{3/2}$		$6d\ ^2D_{5/2}$	
Terms	α_0^1	α_0^1	α_0^2	α_0^1	α_0^2
$\tilde{D}_c$	15.56	15.56	−0.56	15.56	−0.56
$\underline{\tilde{D}_n}$	149.10	167.51	−114.14	128.21	−98.07
$\underline{\tilde{D}_c}$	11.66	11.66	−0.71	11.66	−0.71
$\underline{\tilde{D}_v}\Omega+cc$	0.60	0.21	−0.54	1.03	−1.03
$\underline{\tilde{D}_v}\Lambda_{1n}+cc$	107.74	91.30	−54.32	85.59	−62.17
$\tilde{D}_v\underline{\Lambda_{2n}}+cc$	−4.15	−5.92	−2.84	−4.85	3.68
$S_{1v}\underline{\tilde{D}_v}\Lambda_{1n}+cc$	−5.17	−7.62	4.51	−6.65	5.13
$S_{2v}\underline{\tilde{D}_v}\Lambda_{1n}+cc$	−4.93	−4.64	2.68	−3.44	1.76
$S_{1v}\underline{\tilde{D}_v}\Lambda_{2n}+cc$	−0.02	0.05	0.05	0.02	−0.01
$S_{2v}\tilde{D}_v\Lambda_{2n}+cc$	0.25	−0.18	0.07	−0.15	0.10
Others	0.29	0.61	−0.34	0.64	−0.43
Norm	−1.73	−1.76	1.21	−1.47	1.08

we had also evaluated dipole polarizabilities in the ground and d-metastable states using the sum-over-states approach with the E1 matrix elements from CCSD(T) method and approximated core-correlation and core-valence correlation effects.

In Table IV, we present contributions from individual RCC terms to these results. The trend of the correlation effects in the ground state seems similar to those of Sr$^+$ and Ba$^+$, but due to the presence of core f electrons, the behavior of the correlation effects is a little different for the metastable d-states. The size of core correlation is slightly larger than that of Ba$^+$, but the difference is not as large as it was between Sr$^+$ and Ba$^+$. In contrast to Ba$^+$ where the *ab initio* and sum-over-states results match, we found discrepancies in this system. The discrepancies are mainly because of the inclusion of the doubly excited states in the present work, but there could be cancellations in Ba$^+$ due to which the discrepancies are small.

E. Applications to the optical clocks

All the ions considered in this work are important candidates for optical clocks [3,5,8–10]. There has been an absolute frequency measurement of the $5s\ ^2S_{1/2}\rightarrow 4d\ ^2D_{5/2}$ transition in ^{88}Sr$^+$ by Madej *et al.* [5]. One of the largest uncertainties due to the applied electric field comes from the quadratic Stark shift. In fact, this shift was earlier over estimated due to the large error bars in the calculated dipole polarizabilities of the $5s\ ^2S_{1/2}$ and $4d\ ^2D_{5/2}$ states. Madej *et al.* had used $\alpha_0^1(5s_{1/2})=(1.40\pm0.06)\times10^{-39}$ C^2 s^2 kg^{-1} where we obtain this result as $(1.46\pm0.02)\times10^{-39}$ C^2 s^2 kg^{-1}. The scalar and tensor polarizabilities of the $4d\ ^2D_{5/2}$ were used in [5] as $\alpha_0^1(4d_{5/2})=(8\pm2)\times10^{-40}$ C^2 s^2 kg^{-1} and $\alpha_0^2(4d_{5/2})=(-7\pm2)\times10^{-40}$ C^2 s^2 kg^{-1}, respectively. We obtain these results as $\alpha_0^1(4d_{5/2})=(10.37\pm0.12)\times10^{-40}$ C^2 s^2 kg^{-1} and $\alpha_0^2(4d_{5/2})=(-8.05\pm0.05)\times10^{-40}$ C^2 s^2 kg^{-1}. Using Eq. (2.9) and our results, we obtain the shift rate, which is defined as $\gamma=\frac{\delta(\Delta W_E)}{\delta E^2}$, of the $5s\ ^2S_{1/2}$ state as (1.10 ± 0.01) μHz/(V/m)^2 against (1.06 ± 0.04) μHz/(V/m)^2 of Madej *et al.* Similarly, we obtain $\gamma=(-0.78\pm0.02)$ μHz/(V/m)^2 against results of Madej *et al.* as $\gamma=(-0.6\pm0.2)$ μHz/(V/m)^2 in the $4d\ ^2D_{5/2}$ state using only the scalar polarizability. However assuming the direction of the electric field lies in the z direction, we obtain $\gamma=(-1.27\pm0.03)$ μHz/(V/m)^2, $\gamma=(-0.91\pm0.02)$ μHz/(V/m)^2 and $\gamma=(-0.18\pm0.01)$ μHz/(V/m)^2 for $M=1/2$, $M=3/2$, and $M=5/2$, respectively.

Using Eq. (2.14) and the above results, we also obtain the black-body radiation shift at $T=300$ K in the $5s\ ^2S_{1/2}\rightarrow 4d\ ^2D_{5/2}$ transition in ^{88}Sr$^+$ as (0.22 ± 0.01) Hz and that is an improvement of 10% over the result of Madej *et al.* [5].

It appears that both ^{137}Ba$^+$ and ^{138}Ba$^+$ will be suitable candidates for an optical clock [8,9], but each has some advantages and disadvantages in controlling the systematic errors. For the $6s\ ^2S_{1/2}\rightarrow 5d\ ^2D_{5/2}$ transition in ^{138}Ba$^+$, it would be possible to use techniques similar to the measurement of the frequency in the optical transition in ^{88}Sr$^+$ mentioned earlier. However, one has to encounter the electric quadrupole shift in the $5d\ ^2D_{5/2}$ state for this case. It is possible to overcome this particular shift by considering the possible $F=2(6s_{1/2})\rightarrow F=0(5d_{3/2})$ hyperfine transition in ^{137}Ba$^+$. In this transition, one has to again estimate the possible quadratic Zeeman shifts because of finite nuclear magnetic and quadrupole moments. Our dipole polarizability for the $6s\ ^2S_{1/2}$ state is given by $(2.05\pm0.02)\times10^{-39}$ C^2 s^2 kg^{-1}. The scalar and tensor polarizabilities of the $5d\ ^2D_{3/2}$ state are given by

$(8.05 \pm 0.07) \times 10^{-40}$ C^2 s^2 kg^{-1} and $(-4.06 \pm 0.05) \times 10^{-40}$ C^2 s^2 kg^{-1}, respectively. Similarly, the scalar and tensor polarizabilities of the $5d\ ^2D_{5/2}$ state are given by $(8.35 \pm 0.09) \times 10^{-40}$ C^2 s^2 kg^{-1} and $(-5.09 \pm 0.05) \times 10^{-40}$ C^2 s^2 kg^{-1}, respectively. Due to the choice of the hyperfine transition in ^{137}Ba$^+$, the tensor polarizabilities of these states are zero and hence the polarizabilities of the atomic and hyperfine states are the same. The shift rates are (-1.55 ± 0.01) μHz/(V/m)^2 and (-0.61 ± 0.01) μHz/(V/m)^2 in the $6s\ ^2S_{1/2}$ and $5d\ ^2D_{3/2}$ states, respectively. For ^{138}Ba$^+$, by considering particular M values of the $5d\ ^2D_{5/2}$ state and assuming that the electric field lies in the z direction, we can evaluate the Stark shifts. They are $\gamma = (-0.94 \pm 0.02)$ μHz/(V/m)^2, $\gamma = (-0.71 \pm 0.02)$ μHz/(V/m)^2, and $\gamma = (0.14 \pm 0.01)$ μHz/(V/m)^2 for $M = 1/2$, $M = 3/2$, and $M = 5/2$, respectively. As can be noticed, the result for $M = 5/2$ has opposite sign than other M values. The Stark shifts in these states can be easily estimated using these results for a given applied electric field.

The black-body radiation shift at $T = 300$ K in the $6s\ ^2S_{1/2} \rightarrow 5d\ ^2D_{5/2}$ transition in this system is given as (0.64 ± 0.02) Hz.

Similarly as we had reported earlier [10], both ^{223}Ra$^+$ and ^{225}Ra$^+$ have the same advantages like ^{137}Ba$^+$ and ^{138}Ba$^+$, respectively, for considering as optical clock candidates. In fact, all the low-lying energy levels in these ions are in optical region which will be an advantage for the experimentalists to measure the $7s\ ^2S_{1/2} \rightarrow 6d\ ^2D_{3/2}$ or $7s\ ^2S_{1/2} \rightarrow 6d\ ^2D_{5/2}$ or $F = 2(7s_{1/2}) \rightarrow F = 0(6d_{3/2})$ transition frequencies more precisely than other candidates. Recently, ^{213}Ra whose half-lifetime is around 2.75 m was produced at KVI [34] in the accelerator method and its single ion shares the same advantage with ^{225}Ra$^+$ for becoming suitable candidate for the optical clock. Now assuming that due to the suitable choice of hyperfine states in ^{223}Ra$^+$ [10] like the case for ^{137}Ba$^+$, the tensor polarizability contribution to the Stark shift will be zero and hence using our dipole polarizability results, we obtain the Stark shift rates as (-1.31 ± 0.02) μHz/(V/m)^2 and (-1.05 ± 0.02) μHz/(V/m)^2 in the $7s\ ^2S_{1/2}$ and $6d\ ^2D_{3/2}$ states, respectively. For other isotopes discussed above, by considering particular M values of the $6d\ ^2D_{5/2}$ state and assuming that the electric field lies in the z direction, the Stark shifts are evaluated as $\gamma = (-1.56 \pm 0.03)$ μHz/(V/m)^2, $\gamma = (-1.16 \pm 0.02)$ μHz/(V/m)^2, and $\gamma = (0.29 \pm 0.01)$ μHz/(V/m)^2 for $M = 1/2$, $M = 3/2$, and $M = 5/2$, respectively. The result for $M = 5/2$ has opposite sign than other M values like in ^{138}Ba$^+$. Therefore, the Stark shifts in Ra$^+$ can be estimated accurately using our results for a given applied electric field.

The black-body radiation shift at $T = 300$ K in the $7s\ ^2S_{1/2} \rightarrow 6d\ ^2D_{5/2}$ transition in Ra$^+$ is given as (0.19 ± 0.02) Hz.

From the above Stark shift ratios and BBR shifts in the considered ions, it is found that these systematic errors are small in Ra$^+$ which further supports along with its energy level locations that it will be one of the most suitable candidates for optical clock. In fact, a possible atomic clock with uncertainty in the order of 10^{-17} seems feasible from these results along with the preliminary analysis of Doppler's shifts [35] in Ra$^+$.

V. CONCLUSION

We have employed the relativistic coupled-cluster method to determine *ab initio* results for the dipole polarizabilities of the ground and the metastable d states in the singly ionized strontium, barium, and radium. Electron correlation effects arising through various coupled-cluster terms are given individually and comparative studies are performed for these three ions. Using the results we have obtained, Stark shifts, and black-body radiation shifts for these ions are estimated. Using our results, we were able to reduce the errors of the measured frequency for the optical clock in ^{88}Sr$^+$. Our calculations of the Stark and black-body radiations shifts in both Ba$^+$ and Ra$^+$ could be used to remove the systematic errors in the proposed optical clock experiments for these ions.

ACKNOWLEDGMENTS

This work was supported by NWO under the VENI program with Project No. 680-47-128 and part of the Stichting FOM Physics Program 48 TRIμp. D.M. thanks the Indo-Swedish research grant for research funding. We thank the C-DAC TeraFlop Super Computing facility, Bangalore, India for the cooperation to carry out these calculations on its computers.

---

[1] S. A. Diddams, Th. Udem, J. C. Bergquist, E. A. Curtis, R. E. Drullinger, L. Hollberg, W. M. Itano, W. D. Lee, C. W. Oates, K. R. Vogel, and D. J. Wineland, Science **293**, 825 (2001).
[2] D. Adam, Nature (London) **421**, 207 (2003).
[3] H. S. Margolis, G. P. Barwood, G. Huang, H. A. Klein, S. N. Lea, K. Szymaniec, and P. Gill, Science **306**, 1355 (2004).
[4] W. M. Itano, Phys. Rev. A **73**, 022510 (2006).
[5] A. A. Madej, J. E. Bernard, P. Dubé, L. Marmet, and R. S. Windeler, Phys. Rev. A **70**, 012507 (2004).
[6] T. Schneider, E. Peik, and C. Tamm, Phys. Rev. Lett. **94**, 230801 (2005).
[7] W. H. Oskay, W. M. Itano, and J. C. Bergquist, Phys. Rev. Lett. **94**, 163001 (2005).
[8] J. A. Sherman, T. W. Koerber, A. Markhotok, W. Nagourney, and E. N. Fortson, Phys. Rev. Lett. **94**, 243001 (2005).
[9] J. A. Sherman, W. Trimble, S. Metz, W. Nagourney, and N. Fortson, e-print arXiv:physics/0504013.
[10] B. K. Sahoo, B. P. Das, R. K. Chaudhuri, D. Mukherjee, R. G. E. Timmermans, and K. Jungmann, Phys. Rev. A **76**, 040504(R) (2007).
[11] W. M. Itano, J. Res. Natl. Inst. Stand. Technol. **105**, 829 (2000).
[12] C. Sur, K. V. P. Latha, B. K. Sahoo, R. K. Chaudhuri, B. P. Das, and D. Mukherjee, Phys. Rev. Lett. **96**, 193001 (2006).

[13] B. K. Sahoo, Phys. Rev. A **74**, 020501(R) (2006).
[14] B. K. Sahoo, Phys. Rev. A **73**, 062501 (2006).
[15] B. K. Sahoo, C. Sur, T. Beier, B. P. Das, R. K. Chaudhuri, and D. Mukherjee, Phys. Rev. A **75**, 042504 (2007).
[16] D. Jiang, B. Arora, M. Safronova, and C. W. Clark, J. Phys. B **42**, 154020 (2009).
[17] N. Fortson, Phys. Rev. Lett. **70**, 2383 (1993).
[18] L. W. Wansbeek, B. K. Sahoo, R. G. E. Timmermans, K. Jungmann, B. P. Das, and D. Mukherjee, Phys. Rev. A **78**, 050501(R) (2008).
[19] J. R. P. Angel and P. G. H. Sandars, Proc. R. Soc. London, Ser. A **305**, 125 (1968).
[20] J. W. Farley and W. H. Wing, Phys. Rev. A **23**, 2397 (1981).
[21] W. R. Johnson, *Atomic Structure Theory: Lectures on Atomic Physics* (Springer-Verlag, Berlin, 2007), p. 141.
[22] I. S. Lim and P. Schwerdtfeger, Phys. Rev. A **70**, 062501 (2004).
[23] J. Mitroy, J. Y. Zhang, and M. W. J. Bromley, Phys. Rev. A **77**, 032512 (2008).
[24] P. S. Barklem and B. J. OMara, Mon. Not. R. Astron. Soc. **311**, 535 (2000).
[25] S. H. Patil and K. T. Tang, J. Chem. Phys. **106**, 2298 (1997).
[26] J. Nunkaew, E. S. Shuman, and T. F. Gallagher, Phys. Rev. A **79**, 054501 (2009).
[27] E. L. Snow and S. R. Lundeen, Phys. Rev. A **76**, 052505 (2007).
[28] T. F. Gallagher, R. Kachru, and N. H. Tran, Phys. Rev. A **26**, 2611 (1982).
[29] E. Iskrenova-Tchoukova and M. S. Safronova, Phys. Rev. A **78**, 012508 (2008).
[30] I. Miadoková, V. Kellö, and A. J. Sadlej, Theor. Chem. Acc. **96**, 166 (1997).
[31] B. K. Sahoo, R. G. E. Timmermans, and K. Jungmann, e-print arXiv:0809.5167.
[32] U. I. Safronova, W. R. Johnson, and M. S. Safronova, Phys. Rev. A **76**, 042504 (2007).
[33] Rupsi Pal, Dansha Jiang, M. S. Safronova, and U. I. Safronova, Phys. Rev. A **79**, 062505 (2009).
[34] P. D. Shidling *et al.*, Nucl. Instrum. Methods **A606**, 305 (2009).
[35] K. Jungmann, B. K. Sahoo, R. G. E. Timmermans, O. O. Versolato, and L. W. Wansbeek (unpublished).